INVESTIGATION INTO CAUSES OF RUPTURES OF ELASTOMERIC BEARINGS DUE TO THE GREAT EAST JAPAN EARTHQUAKE

Takeshi Hirose[1], Kaneyoshi Yamada[2]

Abstract

The Great East Japan Earthquake gave rise to considerable ruptures of elastomeric bearings (considering these were designed for the seismic forces of a Level 2 earthquake). This paper, based on the damage results, describes the reasons for the ruptures as analyzed from two perspectives: performance confirmation tests of the elastomeric bearings, and reproduction analysis(dynamic analysis) of earthquake reaction behaviors.

Introduction

The Great East Japan Earthquake of March 11, 2011, caused extensive damage obstructing traffic over broad swaths extending from Tohoku in the north to Kanto. Of particular impact was the damage to the expressways managed by the East Nippon Expressway Company Limited (below, "NEXCO East Japan").

A total of 250 bridges suffered damage, including some which were less seriously hit. Similar to damage seen in the aftermath of the Chuetsu Earthquake of 2004 or the Chuetsu Offshore Earthquake of 2007, damage, in many cases, appeared around the bearings, mainly steel, and on expansion apparatus.

However, on some bridges designed in accord with the 1996 Specifications for Highway Bridges(Sendai East Road/East Viaduct, Sendai North Road/Rifu Viaduct), there was found an unprecedented type of damage: the rupture of elastomeric bearings (considering design earthquake force of a Level 2 earthquake).

This paper focuses on the East Viaduct in reporting on what caused these ruptures.

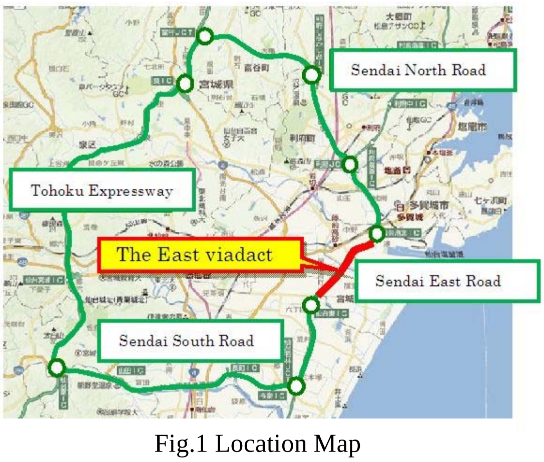

Fig.1 Location Map

State of the Damage

(1) Overview of the Bridges

The East Viaduct is a continuous viaduct with integrated inbound and outbound lanes, made mainly of steel

---

[1] Manager, Technology Planning Section, Technology Department, East Nippon Expressway Company Limited.(NEXCO East), Japan

[2] Senior Structure Advisor, Technology & Procurement Department, Tohoku Regional Head Office, NEXCO East, Japan

continuous box girder or I-section girder extending some 4,390 meters between the Sendai-Higashi IC and the Sendai Kokita IC on the Sendai East Road.

The East Viaduct was constructed as a joint project of the Ministry of Land, Infrastructure, Transport and Tourism with the former Japan Highway Public Corporation, from which NEXCO East is derived. The line has been in service for 10 years since first opening to traffic on August 1, 2001. The rupture of elastomeric bearings due to the 2011 earthquake was confirmed along a widened section of the viaduct at Sendai-ko IC (tentative name), now under construction as a supplemental IC.

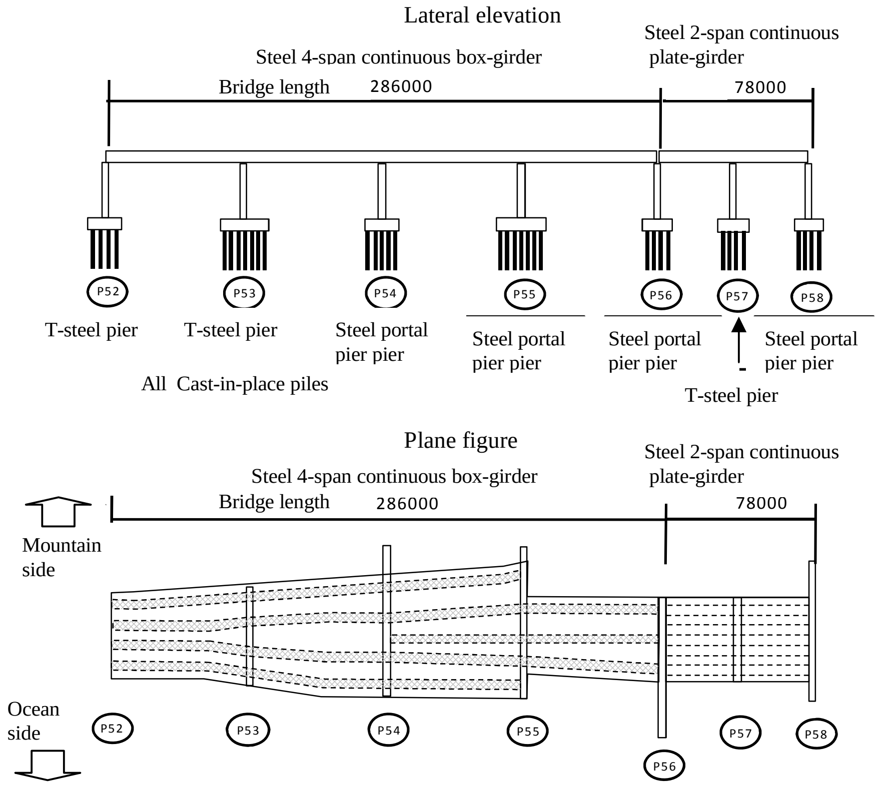

Fig.2 Bridge Diagram (1)

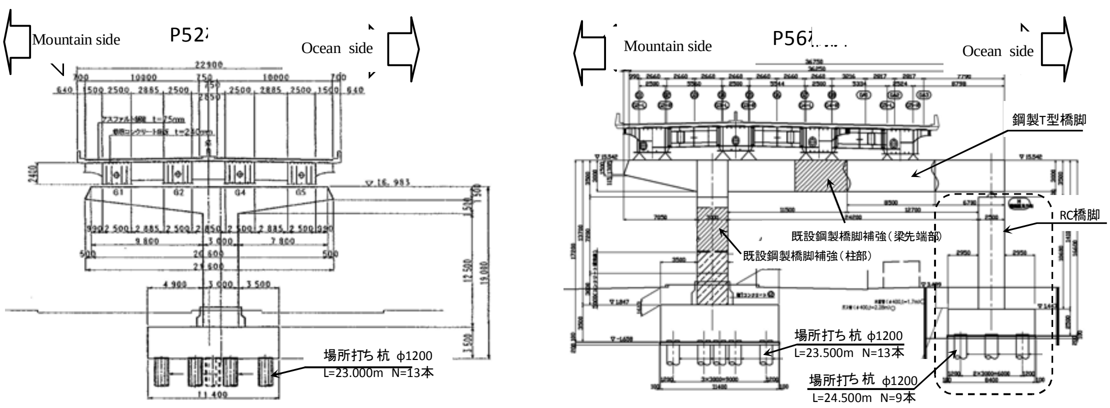

Fig.3 Bridge Diagram (2)

Table 1 Bridge Specifications

Bridge length	4,390 m
Superstructure（Damaged sections）	P52 to P56： Steel 4-span continuous non-composite box-girder（L=285.75m） P56 to P58： Steel 2-span continuous non-composite plate girder （L=77.80m）
Substructure	T-steel: P52,P53,P57 Steel portal rigid (with cantilever beam): P54, P55 Portal type (T-steel + RC column type): P56, P58
Road structure	Class 1, grade 2-B
Ground class	Class II ground
Design load	Live load B
Bearing support conditions	Horizontal earthquake force dispersion type elastomeric bearings
Specification for Highway Bridges	Japan 1996
Date opened	August 1995

Figure 1 shows the location of the viaduct; Figures 2 and 3 are drawings of the bridges whose elastomeric bearings ruptured; Table 1 provides the bridge specifications.

(2) Outline of the damage

The section notable for marked damage to elastomeric bearings extends from pier P52 to pier P58. At the time the earthquake hit, widening work to expand the Sendai-ko IC (tentative name) was underway. It was a structurally complex section where, the width was considerable(integrating inbound and outbound lanes) and variations in width were significant, with piers being of different shapes; there were significant differences in the lengths of adjoining bridge types and girders.

The following are two notable characteristics of the damage to the elastomeric bearings.

1) On the terminal side of pier P52, (right side at top of P52 in Fig.4,below referred to as “P52R”) and on the terminal side of pier P56 (below referred to as “P56R”), all (8) bearings along the bearing support line ruptured.

2) On pier P54 and the terminal side of pier P58 (left side at top of P58 in Fig. 2, below referred to as, “P58L”), only the mountain side bearings ruptured.

There were numbers of joint protectors were installed on each bearing support line (considering the design seismic force of a Level 1 earthquake). Ruptures of the setting bolts of the joint protectors caused many joint protectors to fall out of place. On the other hand, at piers P54 and P55, there was only partial deformation or conditions remained sound.(Fig.4)

The residual displacement at the ruptured elastomeric bearings at P52R was from 9 to 22 mm longitudinally to the bridge axis on the terminal side, and from 144 to 156 mm perpendicularly to the bridge axis on the ocean side. At P56R, the displacement was large, ranging from 0 to 103 mm longitudinally to the bridge axis on the terminal side, and from 562 to 653 mm perpendicularly to the bridge axis on the ocean side. Many had fallen from their shoe seats (vertically about 400 mm).(Fig.5)

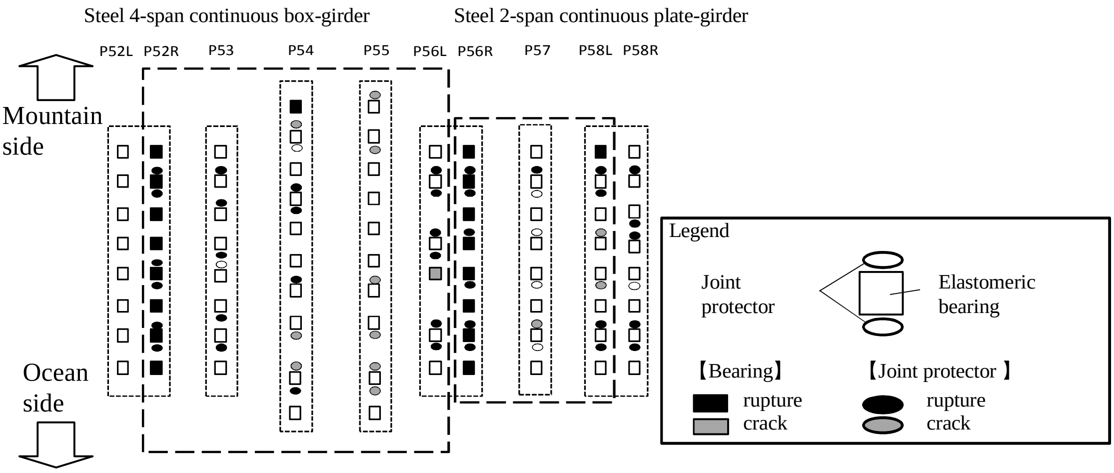

Fig.4 Sites of Bearing Damage

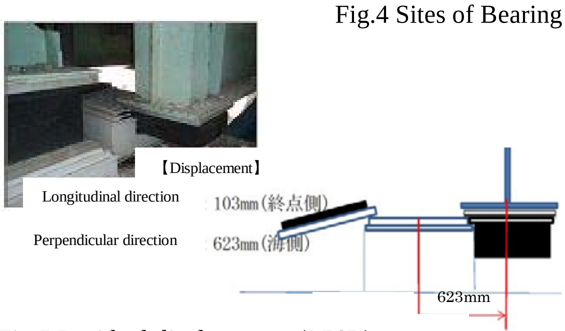

Fig.5 Residual displacement (P56R)

Fig.6 Rupture surface of elastomeric bearing
(P56R S4 bottom surface)

The following are the principal locations of rupture of the elastomeric bearings.
1) P52R: boundary of the rubber and internal steel plates, and near this boundary.
2) P56R: boundary of the rubber and internal steel plate or the end steel plate and near this boundary.

Figure 6 shows the state of the rupture surface of an elastomeric bearing.

Based on the above damage findings, the reasons for the rupture of the elastomeric bearings were analyzed from two perspectives:
1) Testing to confirm the performance of the elastomeric bearings
2) Analysis to reproduce behavior during the earthquake

These analyses were performed in order to clarify if the ruptures were related more to the performance of the elastomeric bearings, or if the response of the bridge to the earthquake was greater than the hypothesized response for the design.

Testing to Confirm the Perfomance of the Elastomeric Bearings

(1) Outline of the Testing

Material testing and shear deformation performance testing of the ruptured elastomeric bearings were conducted. We confirmed that the material properties and the deformation performance of these bearings satisfied the standard values.

Documents have helped confirm that when the elastomeric bearings were manufactured, the products complied with quality control standards and satisfied the standard specification values for their materials, the allowable shear strain,and the design horizontal force.

Some elastomeric bearings which appeared to be undamaged under visual examination (existing bearings) located near the ruptured elastomeric bearings were sampled on the site and tested.

In order to clarify performance differences with the existing bearings, material tables and fabrication methods used at the time of construction were applied to make identical products. The performance verifications testing of the existing bearings (i.e.,those sampled on site) was done using a total of four samples from three points on the East Viaduct (P58L, P58R) and on the Rifu Viaduct (P34). The performance verification testing of the newly fabricated bearings (identical products) used a total of nine newly made bearings of three types each: the East Viaduct (P52R, P56R) and the Rifu Viaduct (P26R).

Table 2 shows the specimen dimensions and numbers tested.

Table 2. Specimen Dimensions and Number Tested

	Bridge name	Locations installed	New or existing	Type of rubber	Rubber shoe product dimensions (Effective dimensions of rubber shoe) (Manufacturer of rubber shoe)	Number tested (Specimen name)	
						Basic properties	Cyclic properties
A	East Viaduct	P52	new	NR (G10)	720×720×t329 (700×700×t29×8layers) (A company)	2 (A1/A2)	1 (A3)
B		P56	new	NR (G10)	520×470×t212 (500×450×t18×7layers) (A company)	2 (B1/B2)	1 (B3)
C	Rifu Viaduct	P26	new	NR (G12)	610×610×t238 (600×600×t20×7layers) (B company)	1 (C1)	2 (C2/C3)
D	East Viaduct	P58L	existing	NR (G10)	520×470×t212 (500×450×t18×7layers) (A company)	1 (D1)	—
E		P58R	existing	NR (G10)	620×570×t240 (600×550×t22×7layers) (C company)	1 (E1)	—
F	Rifu Viaduct	P34	existing	NR (G12)	610×610×t238 (600×600×t20×7layers) (A company)	2 (F1/F2)	—

Table 3. Test Items

Test items		Outline of the test
Basic properties	[1] Compression spring constant Compression displacement	Confirms the compression spring constant and vertical displacement under the design reaction force of elastomeric bearings.
	[2] Shear stiffness	Confirms shear stiffness (3 times ±150%).
	[3] Shear deformation performance	Confirms the elongation performance of rubber materials of elastomeric bearings and the limit of the bonding performance of the rubber and the steel plate. (one-direction loading)
Cyclic properties	[4] Cyclic shear deformation properties	Confirms the elongation performance and the limit of the bonding performance etc. of the rubber and steel plate, of rubber material of elastomeric bearings by cyclic loading
	[5] Test of shear deformation performance after provision of large deformation history.	Performs a one-direction shear deformation performance test after 20 excitation cycles at shear strength of ±200% and ±250%

(Based on NEXCO testing method 418.)

(2) Results of the testing

First, we confirmed that the identical products were successfully reproduced by comparing mill sheets and the material performance test results at the time of construction. The following are the test results.

a) Shear deformation performance testing

Focusing on shear deformation performance from among the basic properties tests presented in Table 3, we here describe the ultimate shear strain, the ultimate horizontal force, and rupture locations. Table 4 shows the results for six elastomeric bearings newly made for the East Viaduct.

The results for specimens A1, A2, and A3 (P52R), show that the ultimate shear strain is below the design allowable value of 250%, and scattering is small. However, the ultimate horizontal force always exceeded the design horizontal force when the shear strain was at 250%.

In the case of specimens B1, B2, and B3 (P56R), the design allowable value of 250% was exceeded, but scattering was widespread. The ultimate horizontal force, as in the case of specimen A, exceeded the design horizontal force at 250% shear strain.

Table 5 shows the results for the three newly made specimens in order to organize the impact of cyclic loading on the ultimate strain.

The data was obtained by performing shear deformation performance testing of C1 after the basic properties test, of C2 after 20 cycles of loading of shear strain at 200%, and of C3 after 20 cycles of loading of shear strain at 250%.

However, the results for C3 show significant decline in the ultimate horizontal force, so these were used as reference values.

Table 6 shows the results of testing of the existing bearings. The ultimate shear strain of all four

Table 4. Test Items

Test results		Specimen No.			A-1	B-1
	[1] One-direction loading (1st specimen)	Ultimate horizontal displacement	δu	mm	540	350
		Ultimate shear strain	γsu	%	233	278
		Ultimate horizontal force	Hu	kN	1532	982
		Ratio to 250% horizontal force (Hu/H)		–	1.25	1.74
		Rupture locations		-	Rubber	Rubber
		Specimen No.			A-2	B-2
	[2] One-direction loading (2nd specimen)	Ultimate horizontal displacement	δu	mm	540	439
		Ultimate shear strain	γsu	%	233	349
		Ultimate horizontal force	Hu	kN	1708	1404
		Ratio to 250% horizontal force (Hu/H)		–	1.39	2.49
		Rupture locations		-	Rubber	Rubber
		Specimen No.			A-3	B-3
	[3] Cyclic loading	Ultimate horizontal displacement	δu	mm	536	360
		Ultimate shear strain	γsu	%	231	286
		Ultimate horizontal force	Hu	kN	1405	930
		Ratio to 250% horizontal force (Hu/H)		–	1.15	1.65
		Rupture locations		-	Rubber	Rubber

■ : Indicates less than 250%

Table 5. Impact of Cyclic Loading on Shear Deformation Performance (newly made bearings)

Test results		Specimen No.			C-2	C-3	C-1
	Large deformation cyclic loading	Shear strain × frequency			200%×20 times	250%×20 times	
		3rd shear spring constant	Ks1	kN/mm	3.436	3.653	
		20th shear spring constant	Ks2	kN/mm	2.892	2.764	
		Difference between 3rd and 20th		%	-15.8	-24.3	
	Shear deformation performance	Ultimate horizontal displacement	δu	mm	377	(391)	417
		Ultimate shear strain	γsu	%	269	(279)	298
		Ultimate horizontal force	Hu	kN	2155	(1352)	2295
		Ratio to 250% horizontal force (Hu/H)		–	2.00	(1.25)	2.12
		Rupture locations		-	Boundary of rubber and steel plate	Rubber	Rubber

Table 6. Results of Testing of Existing Bearings

Test results		Specimen No.			D-1	E-1	F-1
	[1] One-direction loading (1st specimen)	Ultimate horizontal displacement	δu	mm	276	374	292
		Ultimate shear strain	γsu	%	219	243	209
		Ultimate horizontal force	Hu	kN	660	2127	1348
		Ratio to 250% horizontal force (Hu/H)			1.17	2.58	1.25
		Rupture locations			Rubber	Rubber	Rubber
		Specimen No.					F-2
	[2] One-direction loading (2nd specimen)	Ultimate horizontal displacement	δu	mm			351
		Ultimate shear strain	γsu	%			209
		Ultimate horizontal force	Hu	kN			1463
		Ratio to 250% horizontal force (Hu/H)					1.35
		Rupture locations					Rubber

■ : Indicates less than 250%

specimens taken from the East Viaduct and from the Rifu Viaduct did not exceed the design allowable shear strain at 250%. However, the ultimate horizontal force exceeded the design horizontal force at 250% shear strain.

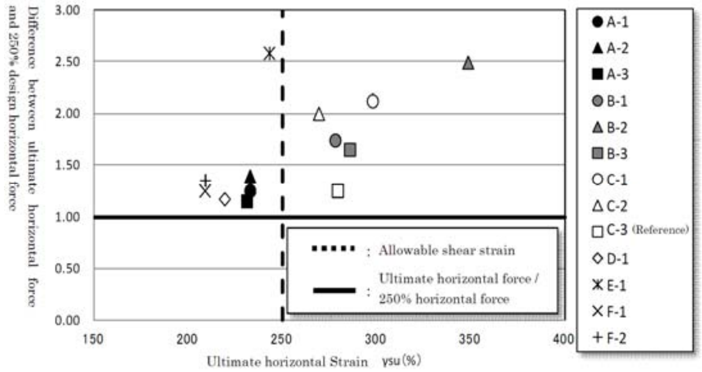

Fig 7. Results of Shear Deformation Performance Testing

b) Analysis of the test results

In results for seven of the 13 specimens, the ultimate shear strain did not exceed the 250% allowable shear strain. The ultimate horizontal force on the other hand, was above the design horizontal force equivalent to the allowable shear strain at 250%.(see Fig.7)

The ultimate shear strain of all of the existing bearings was below the allowable value of 250%. Only specimen A among the newly made bearings was below this level. The reason was attributed to differences in secondary shape factors.

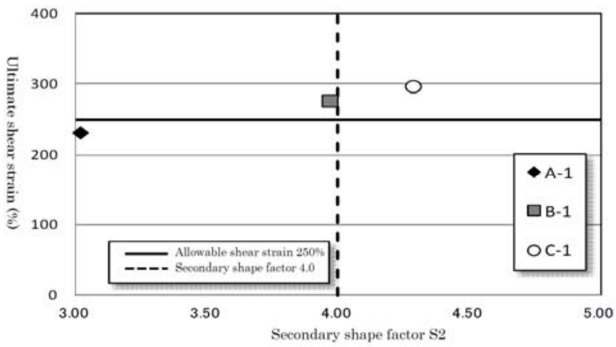

Fig 8. Ultimate strain and the secondary shape factor S2

Figure 8 shows the relationship between the secondary shape factor and ultimate shear strain. The smaller the secondary shape factor the lower the ultimate shear strain. In accord with the 1996 Standards, the secondary shape factor should be 4 or more.

Next, the ultimate shear strains of the newly made bearings and the existing bearings were compared in detail.

Figure 9 shows a comparison of the newly made bearings (C1) with existing bearings (F1, F2). These were elastomeric bearings with identical shapes. Figure 10 shows the comparison of newly made bearings with existing bearings from the same company made of the same material and with identical shapes.

These figures reveal that the ultimate shear strain of the existing bearings was about 20 to 30% below that of the newly made bearings, and that the ultimate horizontal force was reduced by between 30% and 40%.

The cyclic properties are described next.

In order to confirm the impact of the deformation history during a major earthquake, we provided and tested large deformation histories of 20 times ±200%, and 20 times ± 250%.

Specimen C3 partly ruptured at the fourth cycle, so as noted earlier, we used its results as reference values, but a decline in performance was observed (Fig. 11). However, the number of specimens was few, so to clarify the impact of a large deformation history, more data must be sought in the future.

c) Rupture surfaces

The rupture surfaces of the specimens were inside the rubber in 12 of the 13 specimens.However for only specimen C2, which was provided with a large deformation history, the rupture surface was on the steel plate and rubber boundary surface. Figure 12 shows a typical rupture surface.

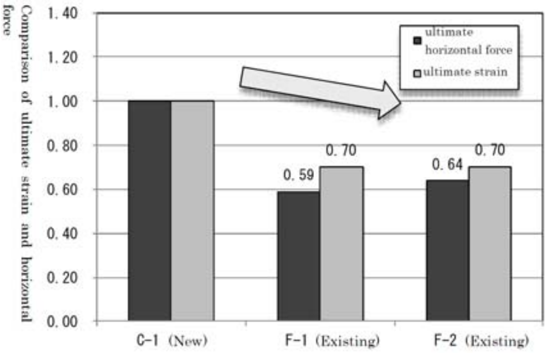

Fig 9. Comparison of Ultimate Shear Strain and Horizontal Force (Same shape)

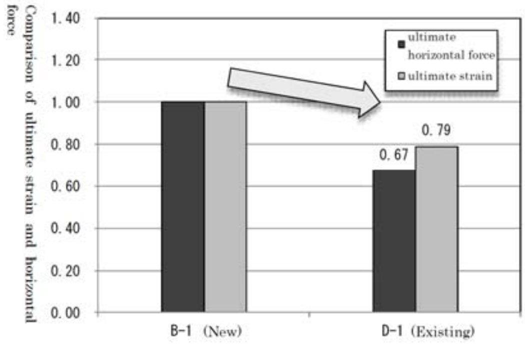

Fig 10. Comparison of Ultimate Shear Strain and Horizontal Force (Same company, same material, same shape)

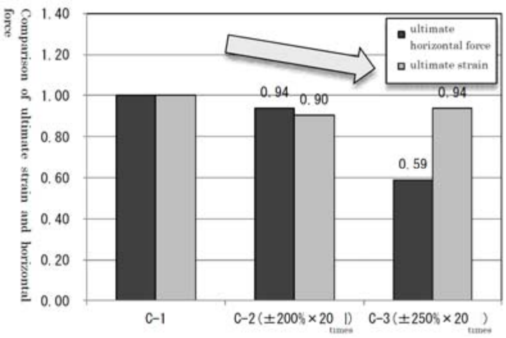

Fig 11. Impact of Large Deformation History

Fig 12. Rupture Surface of Specimens (Left: B1, Right: D1)

Reproduction Analysis

This section reports on the reproduction of behavior during an earthquake using an analysis model based on the damage results.

(1) Entered earthquake motion

We decided to set the Sendai-higashi IC figures as the entered earthquake motion, considering the alignment of ground conditions, the dominant direction of the observed wave form, damage results (main earthquake and aftershocks), etc.

Figure 14 shows the acceleration wave form, the acceleration response spectrum, and the observed wave horizontal component at Sendai-higashi IC on March 11. 2011.

(2) Dynamic analysis

a) Results of analysis using a general model

We analyzed using a general model treating the superstructure as a single beam model. The entered earthquake motion ignores vertical earthquake motion, and the impact of accessories such as expansion devices are not modeled. The results of the analysis are shown in Figure 15.

The results of analysis using the general model differed from damage results, because the response of P52R which ruptured was acctually small, and that of P56L which did not rupture, was larger.

b) Reflecting the state of damage in the model

The modeling was revised based on the analysis of the results of a) and the damage results.

Steel finger joints were installed at P56 and P58, which are piers at the end of girders. Since the fingers of the joints were not broken and there were signs of mutual collision of the fingers on the surfaces of the fingers, the movement in the pependicular direction of the girders could have been constrained by the fingers. (Fig. 16)

The bridge fall prevention structures for the bridge axis direction installed on the widening girders at P56L(newly built part) impacted perpendicularly to the bridge axis with the adjoining elastomeric bearings, causing severe damage. We hypothesized that the movement of the girders perpendicularly to the bridge axis was restricted.(Fig.17)

The joint protectors installed on the bridge were designed for the design horizontal force of a level 1

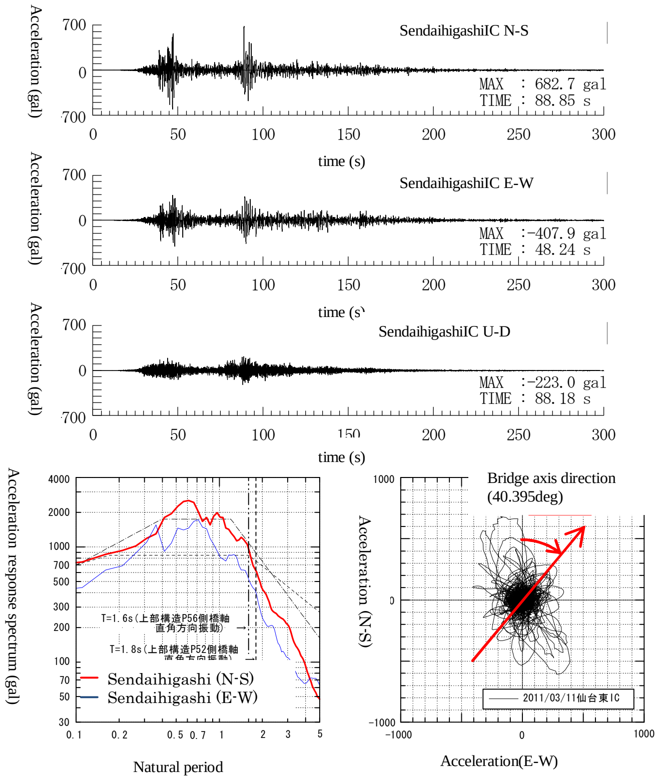

Fig.14 The acceleration wave form / acceleration response spectrum and main direction of observed wave

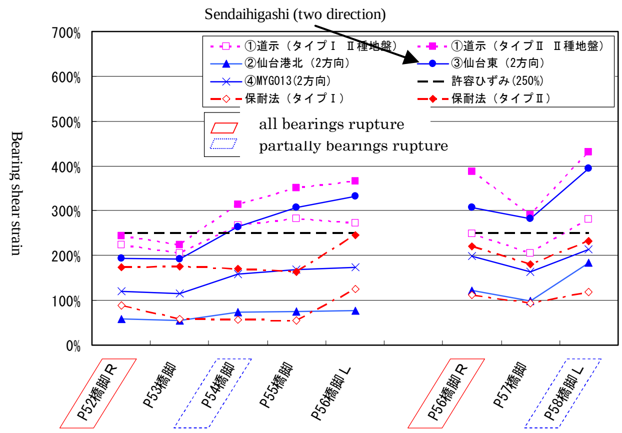

Fig.15 The result of dynamic analysis (perpendicular direction to the bridge axis)

earthquake. Damage to the joint protectors caused by this earthquake can be categorized into three kinds as shown in Figure 18, which were considered in the modeling.

Fig.16 collision of the finger joint

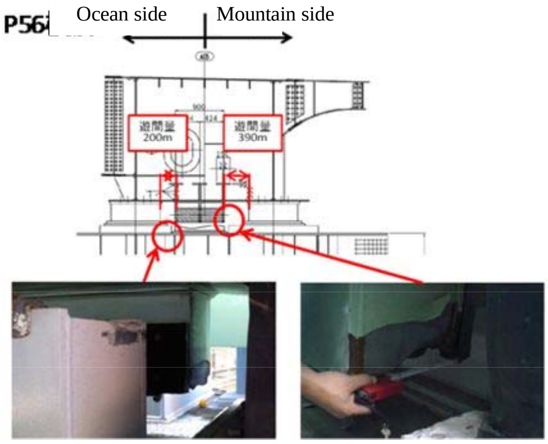

Fig.17 Damage to bridge fall prevention structures (P56L Expanded part)

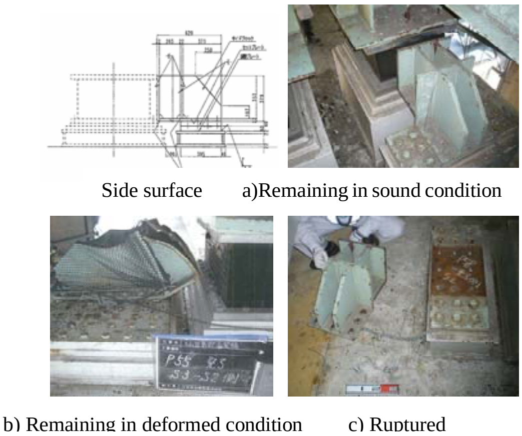

Side surface a)Remaining in sound condition

b) Remaining in deformed condition c) Ruptured

Fig.18 Damage to Joint Protectors

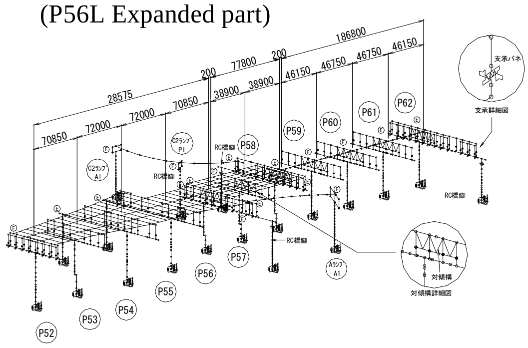

Fig.19 Model Diagram

The results of the shear deformation performance testing of the elastomeric bearings were reflected in the modeling of the bearings. The ruptured bearing capacity was corrected by setting the ultimate shear strain at 230% and the shear spring constant at 1.4 times the design value considering hardening. Figure 19 is the analysis model diagram.

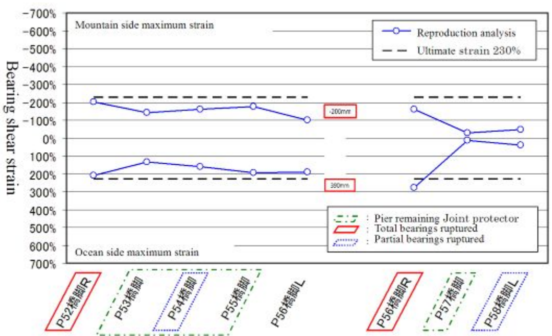

Fig.20 Results of Dynamic Analysis

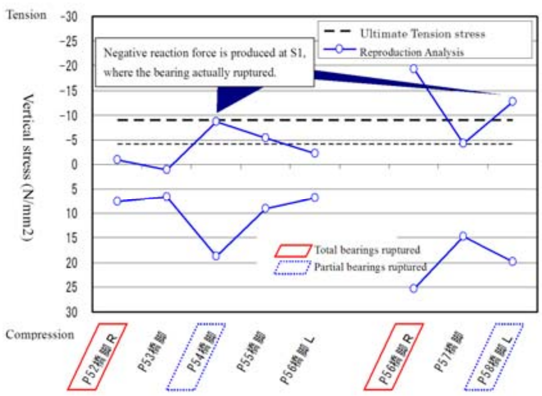

Fig.21 Result of Analysis(Vertical stress of bearings)

c) Dynamic analysis results

Figure 20 shows that the response during the earthquake after modeling to match the results of damage exceeded the ultimate shear strain at P56R, resulted in significant displacement at P52R. Figure 21 shows that at P54 and P58, the response led to a powerful negative reaction force. For these reasons, we decided that the damage results and analysis results are balanced and the modeling is appropriate.

The following is the response during the earthquake based on this analysis.

1) From 43 to 47 seconds after the earthquake

Damage to joint projectors

The main girders impacted the joint protectors adjoining each bearings, and caused damage or deformation.

2) 90.2 seconds after the earthquake

Rupture of entire bearing at P56R

The 1st series of the superstructure, which has heavy bridge girders, followed the 2nd series of the superstructure, which has light girders, through the finger joints. This resulted in rupture of its bearings with small bearing thickness.

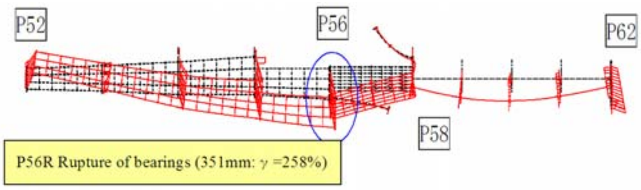

Fig.22 Response Deformation Distribution(T=90.2s)

3) 90.6 seconds after the earthquake

Rupture of P52R bearing

Because girder movement was risticted by the joint protectors remaining on P54 and P55 along with the bridge fall prevention structure on P56 installed on the widened part, the girders rotated in the plane. This caused large deformation at P52R.

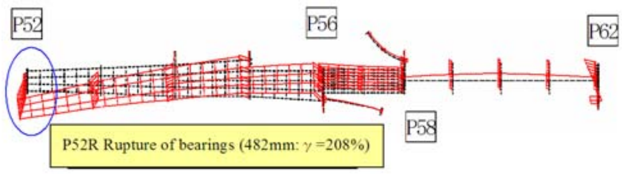

Fig.23 Response Deformation Distribution(T=90.6s)

4) 90 seconds after the earthquake

Rupture of P54 bearing

Stress equivalent to the ultimate tensile stress shown in Figure 21 occurred on bearings installed closest to the mountain side at pier without a cantilever beam.

Rupture of P58L bearing (S1: ruptured at only 1 location)

Figure 24 shows that near P56R-S8 bearing on the 2nd series (P56 to P58), moved horizontally 500 mm to the ocean side and 400 mm downward, and that uplift force affected P58L-S1, which is on a line diagonal to the continuous girders.

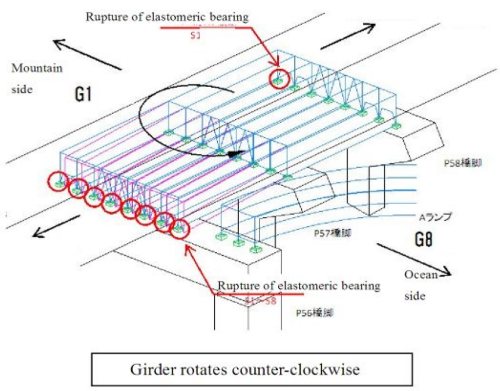

Fig.24 Response Deformation Distribution Diagram (after 90s)

Investigating the Reasons for the Ruptures

We hypothesized the possible reasons for the ruptures based on the results of clarifying the damage to the bridges, the properties of the ruptured elastomeric bearings, and the result of reproduction analysis.

(1) Impact of structural properties and accessories

The reasons for the rupture of the elastomeric bearings concentrated in this section are presumed to lie with the following structural properties.

[1] The types of the bridge and girder lengths of the bridge, in the main line and ramps, differed greatly from those of the adjoining bridge, and the width of these bridges are wide, with great variation at some locations.

[2] There is a mixture of Steel portal piers and T-steel piers.

[3] Accessories which are not modeled for normal design (expansion joints, joint protectors) impacted the earthquake response in various ways.

Although not introduced in the main text, the impact of [1] and [2] on the structural response during an earthquake was clarified by analysis varying the width and varying the shape of the piers. It revealed a tendency for the response of the main structure to increase. We hypothesized that the impact of condition [3] in tandem with [1] and [2], might produce a more complex vibration mode during the earthquake, and that this caused the rupture of the elastomeric bearings.

The following are hypothesized to be the reasons for rupture in each case.

(2) Reasons for ruptures of each location

a) P56R bearing

The superstructure, which has heavy bridge girders, followed the adjoining superstructure, which has light girders, through the finger joints, causing rupture of its bearings with small bearing thickness. (Figure 25, Table 7).

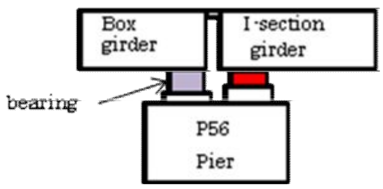

Fig.25 Different height of the bearings on P56

Table.7 Rubber Layer Thickness (mm)

Pier No	Bearing No	Total thickness of the rubber layer (mm)
P56L	S1～S8	264
P56R	S1、S8	136
	S2～S7	126

b) P52R bearing

Because the movement of the girders was limited by the joint protectors remaining on P54 and P55 and the bridge fall prevention structure installed on P56 on the widened part, the girders rotated in the plane. This caused large deformation of P52R. (Fig. 23) The response of shear strain during the earthquake was lower than the ultimate shear strain. However, the age-related deterioration of the elastomeric bearings could have lowered the shear deformation performance, resulting in the rupture.

c) P54, P58 bearings (mountain side)

Because the superstructure is wide and there are mixed pier forms (T-shaped piers, and on the ocean side, portal piers with cantilever beams), torsional rotation deformation mode was seen in the girders, causing stress equivalent to tensile rupture shown in Figure 21, in the bearings without cantilever beams closest to the mountain side. Static analysis performed treating the residual displacement of P56R, P57, and P58L as forced displacement to apply to the superstructure from P56 to P58, confirmed that tensile stress of -50N/mm was produced in bearings at P58 closest to the mountain side, greatly increasing the stress equivalent to tensile rupture. (Fig. 26)

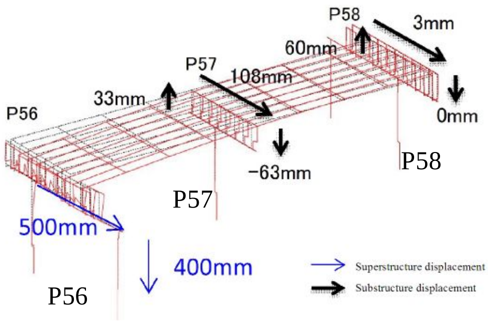

Fig.26 Residual displacement

(3) Differences between rupture surfaces

The rupture surfaces of the elastomeric bearings by the earthquake were nearly all at the bonding boundaries between the rubber and steel plates. However, the rupture surfaces in the shear deformation performance testing was different from those occurring inside the rubber in 12 of the 13 specimens.

The test could be done as one-direction loading at constant speed (10mm/sec) and constant surface pressure (equivalent to dead load), however it is assumed that during the earthquake, behavior was complex, force also acted vertically, and the duration was long.

For the above reasons, it is predicted that the performance of the elastomeric bearings during an earthquake will show smaller values than those obtained by testing.

Conclusion

Based on the damage results, the reasons for rupture of elastomeric bearings were analyzed from two perspectives: performance confirmation testing of the elastomeric bearings and reproduction analysis of behavior during the earthquake. The following are the results.

1) Performance confirmation testing of the elastomeric bearings

[1] The ruptured elastomeric bearings were products which satisfied quality control standards of the time they were manufactured, and had the design allowable shear strain and the design horizontal force.

[2] On the existing bearings, the ultimate horizontal force and the ultimate shear strain were both lower than those of the newly made bearings.

[3] On the newly made bearings, the ultimate horizontal force and the ultimate shear strain both tended to fall under large deformation history.

[4] The locations of rupture of the ruptured elastomeric bearings were at the bonding

boundaries between the rubber and steel plates, however the rupture surfaces in the shear deformation performance testing were almost all inside the rubber. In a case, the rupture surface of the elastomeric bearing under large deformation history was on the bonding surface boundary between the rubber and steel plates.

The above means that it is difficult to accurately evaluate the performance of the elastomeric bearings during an earthquake because of restrictions on the testing apparatus (surface pressure, loading velocity, etc.). It is also undeniable that only a few specimens were tested and the bearing manufacturers were limited. It is necessary to clarify factors such as the relationship of the material testing and product performance, the age-related deterioration, impact of secondary shape factors, and that of the large deformation history etc. based on a larger quantity of data.

2) Results of reproduction analysis of behavior during the earthquake

The reasons for the rupture of the elastomeric bearings concentrated in this section are presumed to be the following structural properties.

[1] The types and girder lengths of the bridge, in the main line and ramps, differs greatly from those of an adjoining bridge, and the width of these bridges are wide, with meaningful variations at some points.

[2] Steel portal piers and T-steel piers are mixed.

[3] Accessories not modeled for normal design impacted the earthquake response in various ways.

Factor not considered by the design are the fact that the superstructure, which has heavy bridge girders, followed the other superstructure, which has light girders, through expansion jonits (finger joints). This caused rupture of the bearings with small bearing thickness. The restrictions on the movement of the bridge fall prevention structures and the joint protectors also caused serious displacement of the bearings.

Acknowledgement

The damage to these laminated elastomeric bearings of bridges was studied by the Great East Japan Earthquake East Viaduct/Rifu Viaduct Damage Restoration Study Committee (Chairman: Professor Motoyuki SUZUKI, of Tohoku University), a committee of scholars formed to clarify the reasons for the ruptures and to propose restoration methods. The committee members have provided valuable insights, with input and guidance from a variety of perspectives. We are deeply grateful for their many contributions.

References

1) Specifications/Commentaries for Highway Bridges December 1996, V. Seismic Design
2) Specifications/Commentaries for Highway Bridges March 2002, V. Seismic Design
3) Manual for Bearings of Highway Bridges, July 1991
4) Manual for Bearings of Highway Bridges, March 2004